Williamsburg, Virginia
ACTIVE 04
2004 September 20-22

Global Active Control Of Tonal Noise From Small Axial Cooling Fans

Brian B. Monson, Scott D. Sommerfeldt
Brigham Young University
BYU N203 ESC
Provo, UT 84602
brianbmonson@byu.net

ABSTRACT

An active noise control system has previously been developed for the reduction of tonal noise radiated by small axial cooling fans, such as those found in desktop computers. This system uses four small actuators surrounding the fan in a mock computer casing. Due to industry volume constraints, a smaller fan and speaker configuration is desirable. If the smaller configuration is able to maintain similar control performance, as well as cooling performance, it is anticipated that practical application of the control system could be widespread. The smaller control system employs a smaller fan running at a higher speed, generating greater output noise levels at higher frequency tones. Global attenuation of these levels is desired. Experimental results of the system will be presented. A comparison of the two systems, including overall global control performance, will be discussed.

1. INTRODUCTION

The active control of noise radiated by small axial cooling fans has received some recent scientific attention, particularly with regard to those cooling agents found in standard electronic office equipment, such as desktop computers. High levels of noise radiated from these fans are found in the workplace, the home, and the classroom. Such levels can be disturbing or distracting and cause an unnecessary annoyance. Prolonged exposure to even low levels of such office noise can be detrimental to both health and well being.[1]

Fan noise is characterized as both broadband and tonal in nature, as can be seen in Figure 1. The broadband component of the noise has received relatively little scientific attention, but has been attributed to unsteady time-variant fluid loading on the blades of the fan as it rotates.[2] Tonal noise is caused by unsteady time-invariant fluid loading on the rotating fan blades. The latter may be ascribed to the placement of stationary flow obstructions near the inlet or exhaust of the fan, such as stators or finger guards. The tones present in the fan noise spectrum are found to be harmonically related to each other, and directly related to the rotational speed of the fan. The first major tone, referred to as the blade passage frequency (BPF), typically lies between 100 and 600 Hz and generally exhibits the highest radiation level. The blade passage frequency is calculated from revolutions per minute as

$$BPF = N \times \frac{RPM}{60}, \tag{1}$$

where N is the number of blades on the fan. While both noise components mentioned are present in the spectrum of cooling fan noise, the tonal component typically dominates the overall sound pressure level and perceived noise level. It has therefore been the emphasis of most studies done on fan noise control.

Active noise control has become an attractive solution for the reduction of fan noise as developments in digital signal processing have allowed active methods of control to become more viable. Notable efforts have been made to combat the axial fan noise problem, with some success, by Quinlan[3], Wu[4], and Lauchle, *et al.*[2] These studies examined single channel control for the blade passage frequency and its harmonics. A more recent study performed by Gee and Sommerfeldt[5] showed that multi-channel control exhibited good global noise reduction of the blade passage frequency and its harmonics for an 80 mm DC fan. This control system was based on a multi-channel version of the filtered-x LMS algorithm, developed by Sommerfeldt.[6] A detailed description of this algorithm may be found in reference 6, and is therefore not included in this paper. There are two points of particular significance in the control approach taken by Gee and Sommerfeldt that distinguish it from work done previously. That is, 1) the study employed multi-channel adaptive control, whereas previous efforts were concentrated on single channel control, and 2) the study showed that near field error sensor location is a possible and stable method of fan noise

control, and, in fact, that an optimized location for these error sensors exists in the same plane as the fan and control actuators such that optimum global control may be achieved. It is the research done by Gee and Sommerfeldt that becomes the basis for the current research.

The 80 mm fan referred to earlier is a standard size for desktop computer cooling applications. The fan with the control system embedded, however, requires an area of 125 x 125 mm. With increasing efforts to decrease the size of desktop computers, a control and fan configuration that fits within the standard 80 x 80 mm area is desired for a more commercially viable system. The selection of a 60 mm DC fan was made to comply with this spatial constraint. The current objective is to determine if a smaller fan and control system is able to demonstrate similar control performance to that of the original system. Performance of the smaller control system and a comparison of the 60 mm fan configuration to that of the 80 mm fan follow.

2. EXPERIMENTAL APPARATUS

A mock computer casing constructed at Brigham Young University was used for the research. The aluminum casing, shown in Figure 2, is approximately 0.45 m in height, 0.4 m in length, and 0.25 m in width. The control arrangement for the 80 mm fan (also seen in Figure 2) consisted of four 29 mm loudspeakers located coplanar with and surrounding the fan. The 60 mm control arrangement, embedded in the top wall of the casing, is seen in Figure 3. Four miniature loudspeakers, 20 mm in diameter, were selected as control actuators. The control sources are spaced symmetrically around the 60 mm fan, fitting within an 80 x 80 mm area. Miniature loudspeakers present a problem in that their low frequency response is generally poor, and input voltage to the loudspeakers must be limited. With typical blade passage frequencies found below 1000 Hz, it is essential for effective control that control actuators have a good response in this region. To improve the response of the loudspeakers, each is enclosed separately within the computer casing by a small plastic enclosure, creating a traditional bass-reflex system.

Located on the 60 mm fan are seven blades and three support struts. The fan is run at a constant voltage, near 10 V, giving an approximate rotational speed of 5140 revolutions per minute. A small aluminum obstruction is placed directly behind the fan to simulate possible stationary obstructions found in a computer casing. An electronic infrared emitter/detector pair placed on either side of the fan is used to determine the blade passage frequency and serves as a reference signal for the feed-forward adaptive control algorithm discussed previously. Four mobile precision microphones are used as error sensor inputs for the control algorithm, placed on the surface of the casing.

All measurements were taken in an anechoic chamber located on the Brigham Young University campus. Figure 4 shows a rotating semicircular boom used to the measure sound pressure level at equally spaced points away from the casing. The boom is 3.1 m in diameter, and precision microphones are placed at 15-degree increments around the boom. The boom was rotated clockwise in ten 18-degree increments to obtain a total of 143 data points for each global sound pressure measurement.

The filtered-x LMS algorithm was implemented using a Spectrum 96000 floating-point digital signal processing board, mounted in a computer with a 486 processor. The sampling frequency was kept at 4 kHz for all measurements shown of the 60 mm system. The control outputs from the computer were low-pass filtered at 2 kHz to prevent aliasing from occurring. The computer and DSP hardware were located in a control room separate from the anechoic chamber, so that all measurements and control tests were performed remotely.

3. THEORETICAL MODELING

A. Mutual Source Coupling

Typically, if the principle of mutual coupling can be employed in the active control of a noise source radiating into free space, the resulting control behavior is of a more global nature, and is therefore more desirable. While an extensive discussion of source coupling is not the intention of this paper, a brief summary of the theory involved is an appropriate segue for the discussion that follows.

It has been shown[7,8] that as two monopole sources radiating into free space are brought into near-field proximity with one another, the mutual impedance seen by each source is modified due to the presence of the other source, and the total power, W, radiated by both sources is determined analytically to be

$$W = \frac{k^2 \rho c}{8\pi} |Q_1|^2 \left[1 + A^2 + 2A \operatorname{sinc} kd \cos\gamma\right], \tag{2}$$

$$A = \frac{|Q_2|}{|Q_1|}, \quad \gamma = \textit{complex phase difference}.$$

where k is the acoustic wave number, ρ is the density of the medium (kg/m^3), c is the speed of sound (m/s), and d is the separation distance (m) between the two sources. Q_1 and Q_2 are the monopole source strengths. Optimizing the secondary source strength, Q_2, relative to the primary source strength, Q_1, and minimizing the above equation leads to the minimum power radiated by both sources,

$$W_{MIN} = \frac{k^2 \rho c}{8\pi} |Q_1|^2 \left[1 - \mathrm{sinc}^2(kd)\right]. \tag{3}$$

This expression is found to differ only slightly from the radiated power of a dipole,

$$W_{DI} = \frac{k^2 \rho c Q^2}{8\pi} 2\left[1 - \mathrm{sinc}(kd)\right], \tag{4}$$

due to the manipulation of the secondary source strength. On the right side of equation (3) is seen the expression representing the power radiated by a single monopole source of strength Q_1, so that W_{MIN} may also be expressed as

$$W_{MIN} = W_{MONO}\left[1 - \mathrm{sinc}^2(kd)\right]. \tag{5}$$

B. Control Configuration

Modeling the fan and control actuators as point monopole sources results in a control configuration consisting of a single monopole noise source surrounded by four symmetrically spaced control sources. Following a similar, though considerably more complex, procedure as above, such configurations have been studied by Nelson, *et al.* and others,[9] and the minimum possible power radiation has been analyzed. The minimum power radiation, relative to the power radiation of a single monopole, is plotted in Figure 5 as a function of *kd*. For the 60 mm fan configuration, the separation distance is 0.045 m, measured from the center of the fan to the center of the control loudspeaker. Although the analysis shown was carried out for the free-field case, the relative strengths of the noise source and control sources for the current application, as well as the minimum power radiation plot, are identical to the free-field case, in that the presence of a baffle simply scales all source strengths by a factor of two.

From the plot it can be seen that as *kd* becomes very small, radiated power is greatly decreased, whereas *kd* approaching π leads to very little or no reduction of radiated power. It is interesting to note that as *kd* becomes small there also appears to be very little difference in the curves depicting the attenuation for the three, four, and eight control source configurations. The four control source and eight control source curves appear to be nearly identical. The decision to use four control sources is based on the premise that employing four symmetrically spaced sources, rather than eight, decreases both material cost and necessary computation time, with negligible loss of control performance. A three source configuration should behave similarly to a four source configuration, and the same argument applies that such an arrangement would be less materially and computationally expensive. However, given the motivations behind this research, the four source configuration was implemented for straightforwardness in developing a configuration capable of fitting into the 80 x 80 mm area. A future study of the performance of a system with three control sources is anticipated.

C. Error Sensor Location

Error sensor microphone placement may be optimized by finding the regions of greatest pressure attenuation when the global sound power radiation is minimized.[8] An analysis of such regions located in the same plane as a baffled source and four symmetrically spaced control sources[9] can be seen in Figures 6-7. Each plot shows the controlled pressure field, relative to the noise source strength, with the dark closed line representing a pressure null. This null shape varies slightly depending upon frequency and separation distance from the noise source and control sources. Figure 6 represents the 600 Hz case (the blade passage frequency of the 60 mm fan) with a separation distance of 0.045 m. Figure 7 shows the attenuation of an 1800 Hz frequency (3 x BPF) with the same separation distance. An optimum location for error sensors may be found by graphically locating points that are common to null curves for all frequencies of interest. This method, however, is not without its limitations in a practical application. In the case of fan noise active control, for example, positions must be selected that are sufficiently far from the fan to achieve an acceptable signal-to-noise ratio. Placing sensors too close in proximity to the fan causes an increase in noise due to airflow across the microphone diaphragm.

With these considerations, several experiments were conducted with different error sensor locations, and the results analyzed. Graphically, a location was chosen beforehand of 5 cm from the center of the fan in the direction toward the center of the control loudspeaker, and 2.5 cm in the perpendicular direction. These coordinates were repeated for each error sensor relative to 0-, 90-, 180-, and 270-degrees from the fan axis. Sensors placed in this arrangement gave the best control performance of all measurements taken. These results are discussed more specifically in the next section.

4. EXPERIMENTAL RESULTS

A. Global Results

For the 80 mm fan, the blade passage frequency is 370 Hz (see Figure 1), and its first few harmonics are present in the noise spectrum. Figures 8-10 show plots of the previous reduction achieved with the first three harmonics of the 80 mm fan control system. For each harmonic the mean-square pressure reduction (MPR) is calculated according to the formula

$$MPR_f\ (dB) = 10\log \frac{\sum_{n=1}^{N} p_{OFF}^2(x_n)}{\sum_{n=1}^{N} p_{ON}^2(x_n)}\ , \tag{6}$$

where N is the total number of data points measured and the subscript f represents the frequency of interest. The subscripts *OFF* and *ON* denote the pressure with active control off and active control on. In the plots, the mesh surface represents the sound pressure level of the fan radiating without active control, and the solid surface is the radiation with control running. The plots give global sound pressure level measurements in dB re 20 μPa, with increased pressure indicated by both increasing spherical radius and color scale. In interpreting the plots, it is important to remember that the fan and control system are raised 0.45 m above the ground, which leads to a skewing of the pressure levels toward the positive z-direction. For the first three harmonics, the control system achieved mean-square reductions of 10.1 dB, 16.1 dB, and 12.8 dB, respectively.

The blade passage frequency for the 60 mm fan is 600 Hz, with the second and third harmonics at 1200 Hz and 1800 Hz. Global reduction plots of the 60 mm fan noise are shown in Figures 11-13. The mean-square pressure reductions, calculated as before, are found to be 14.9 dB, 18.9 dB, and 10.5 dB for the fundamental, second, and third harmonic, respectively. It is interesting to note that the mesh surfaces reveal the omnidirectional behavior of both fans' blade passage frequencies without control. This suggests monopole-like characteristics.

B. Comparison

At this point, a comparison of the two systems is appropriate. It is seen from the graphs that the two systems demonstrate similar control performance. Both are able to achieve good global control of the first three harmonics of the fan BPF, though attenuation of the BPF itself is notably less than the second harmonic. Perhaps the greatest difference between the two systems is seen in the control of the blade passage frequencies. There exists a small region in the 370 Hz plot where the sound pressure level is seen to actually increase with active control running, though the overall reduction was still significant. This may possibly be attributed to a poor loudspeaker frequency response at 370 Hz for one or more of the control loudspeakers existing in that region. This argument is strengthened by noting that though the control loudspeakers for the 60 mm system are smaller in diameter, the increase of frequency to 600 Hz seems to have eliminated the problem.

The 60 mm system, however, does not achieve flawless control of the blade passage frequency either. This is seen in the considerable increase of attenuation from the BPF to the second harmonic. Such an increase is counter-intuitive when considering the analysis by Nelson, *et al.* An increase in frequency leads to an increase in *kd*, which implies a decrease in attenuation. It is deduced, then, that the fundamental is not being attenuated as much as is ideally possible. A comparison to the minimum power radiation plot confirms that this is indeed the case. The 600 Hz tone produces a *kd* value of 0.5, which dictates an attenuation of close to 30 dB in the ideal case. It is likely that the 14.9 dB reduction may be attributed to poor actuator low frequency response at 600 Hz. To verify this suggestion, a total harmonic distortion analysis has been done, and preliminary results show that nonlinearities arise when driving the miniature loudspeakers at 600 Hz.

In the case of the second harmonic, attenuation at 1200 Hz (60 mm fan) is 2.8 dB greater than at 740 Hz (80 mm fan). Here, too, suspicion of poor low frequency response arises in the 80 mm control instance. A comparison to the theoretical ideal for the second harmonic is instructive. At 1200 Hz, *kd* is calculated to be 1, giving an attenuation of 22 dB – 3 dB greater than that achieved experimentally. A similar analysis follows for the third harmonic. In this case, however, the attenuation at 1110 Hz in the 80 mm system is 2.3 dB greater than the 1800 Hz of the 60 mm system. This may be expected, as the *kd* value increases from 1.2 to 1.5 with the increase in frequency. Comparison to the minimum power radiation shows that the attenuation at 1800 Hz is 3 dB less than the theoretical ideal. The harmonic distortion present when driving the control loudspeakers at 600 Hz may give some clarification on why these theoretical ideals are not met. Table 1 outlines the comparison of *kd* values and attenuations of the two systems versus the theory developed by Nelson, *et al.* While not yet achieving ideal values, reduction of the second and third harmonics in the 60 mm fan system appears to approach the predicted ideal.

5. CONCLUSIONS

The 60 mm fan control system appears to exhibit similar control performance to that of the 80 mm fan control system developed by Gee and Sommerfeldt. This suggests that replacement of an 80 mm fan with the 60 mm fan and control system seems to be a feasible step toward making active control a more practical method of reducing axial cooling fan noise. With the 60 mm fan and control actuator configuration meeting the spatial constraint of an 80 x 80 mm area, the need for manipulation of current electronic equipment design is minimal. A retrofit option may even exist for equipment already manufactured and distributed.

While not yet ideal, it appears that the theoretical predictions accurately depict the control configuration used in the 60 mm control system. Improvements upon the system are also anticipated in the future. Of perhaps greatest significance, the optimization of the miniature loudspeaker enclosures is necessary for control of the blade passage frequency. Replacement of the precision microphone error sensors with smaller electret microphones is needed. Currently, limitations on the digital signal processing chip constrain the sampling frequency to 4 kHz. Employment of a faster DSP chip should allow for more rapid computation and sampling rate, and, with this change, the fourth harmonic of the BPF may also be controlled. The current research has not yet attempted to control the broadband component of the fan noise. If sufficient control is demonstrated with the tonal noise, the broadband noise will become dominant. Efforts may then be focused on decreasing the broadband noise using active control.

A plenum is currently under construction at Brigham Young University, following the ISO standard.[10] The use of the plenum will allow for standardized acoustical measurements of noise generated by the fan (e.g. sound power). The airflow characteristics of the 60 mm fan also require further study. Preliminary measurements indicate that the 60 mm fan running at 10 V is able to output close to 90 percent of the 80 mm fan airflow. Techniques used in airflow measurement are being examined for an accurate test to be performed.

6. REFERENCES

1. G. W. Evans and D. Johnson, "Stress and open-office noise," *J. Applied Psychology,* **85**, 779-783 (2000).

2. G. C. Lauchle, J. R. MacGillivray, and D. C. Swanson, "Active control of axial-flow fan noise," *J. Acoust. Soc. Am.* **101**, 341-349 (1997).

3. D. A. Quinlan, "Application of active control to axial flow fans," *Noise Control Eng. J.* **39**, 95-101 (1992).

4. Mei Q. Wu, "Active cancellation of small cooling fan noise from office equipment," *Proc. INTER-NOISE 95,* edited by Robert J. Bernhard and J. Stuart Bolton, Vol. 2, pp. 525-528, 1995.

5. Kent L. Gee and Scott D. Sommerfeldt, "A compact active control implementation for axial cooling fan noise," *Noise Control Eng. J.* **51** (6), 325-334 (2003).

6. Scott D. Sommerfeldt, "Multi-channel adaptive control of structural vibration," *Noise Control Eng. J.* **37**, 77-89 (1991).

7. P. A. Nelson and S. J. Elliott, *Active Control of Sound* (Academic, London, 1992).

8. Colin H. Hansen and Scott D. Snyder, *Active Control of Noise and Vibration* (E & FN Spon, London, 1997).

9. Kent L. Gee and Scott D. Sommerfeldt, "Application of theoretical modeling to multichannel active control of cooling fan noise," *J. Acoust. Soc. Am.* **115** (1), 228-236 (2004).

10. *Acoustics—Method for the measurement of airborne noise emitted by small air-moving devices,* International Standard ISO 10302 (International Organization for Standardization, Geneva, Switzerland, 1996).

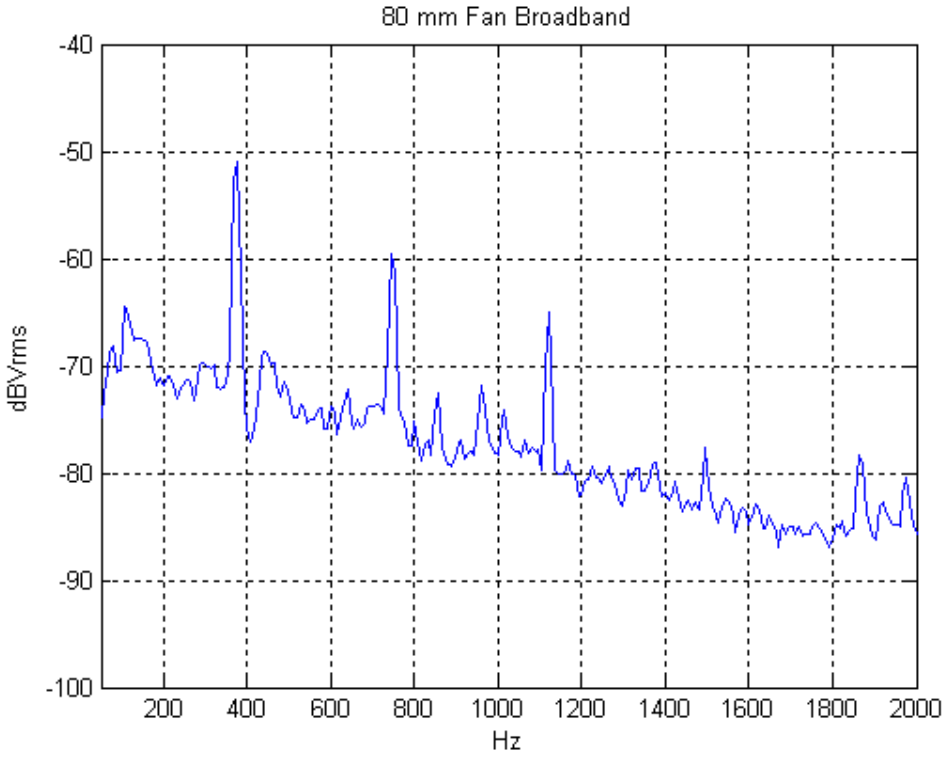

Figure 1. A typical power spectrum of fan noise consisting of both broadband and tonal noise.

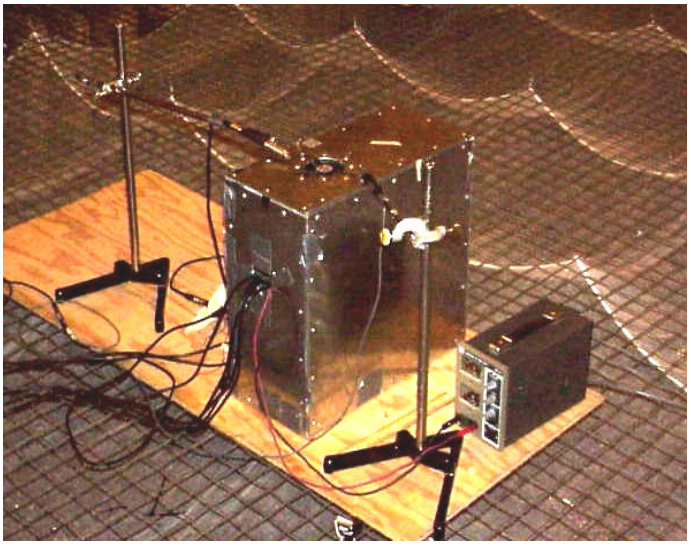

Figure 2. An aluminum mock computer casing containing the 80 mm fan and four 29 mm loudspeakers.

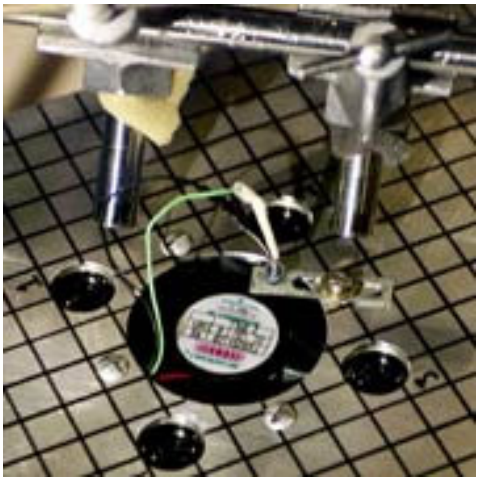

Figure 3. The 60 mm fan surrounded by four 20 mm miniature loudspeakers.

Figure 4. A rotating semicircular microphone boom located in the anechoic chamber on the Brigham Young University campus.

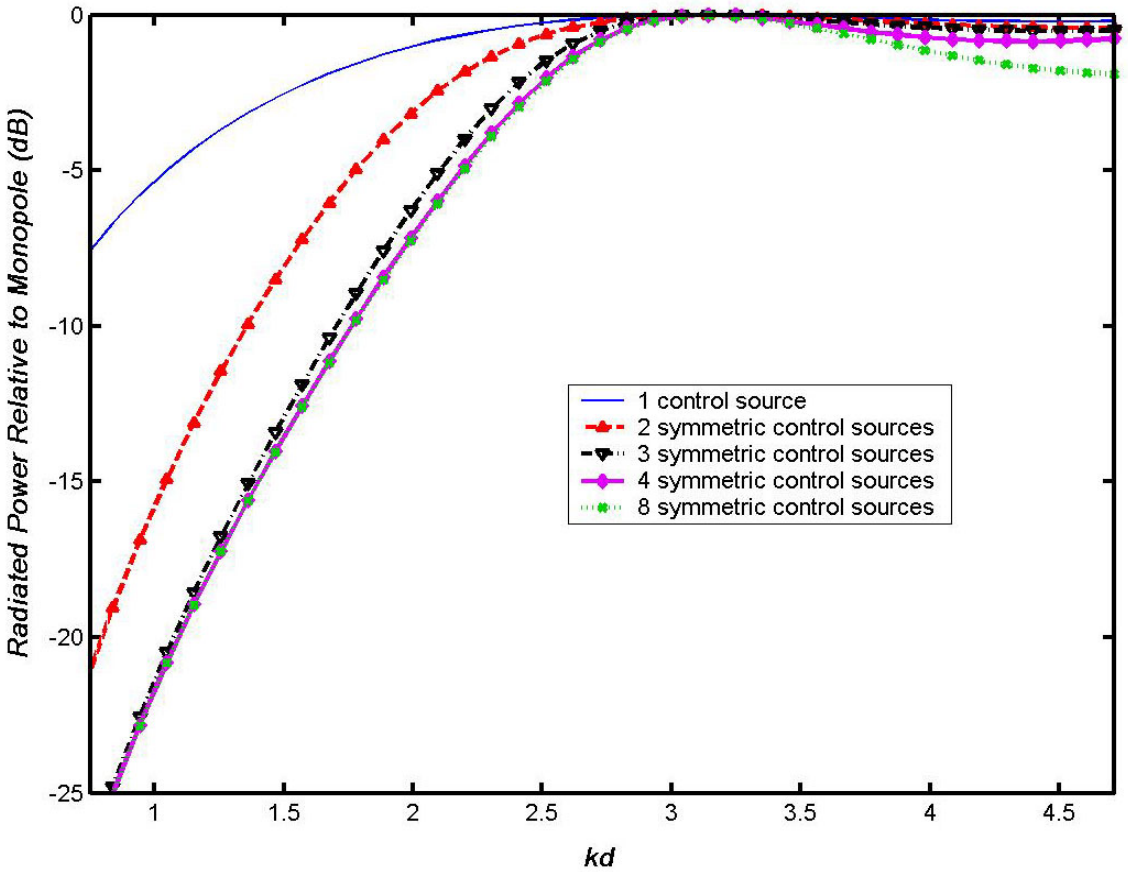

Figure 5. Minimum radiated power for control source arrangements of 1, 2, 3, 4, and 8 symmetrically spaced sources, developed by Nelson *et. al*.

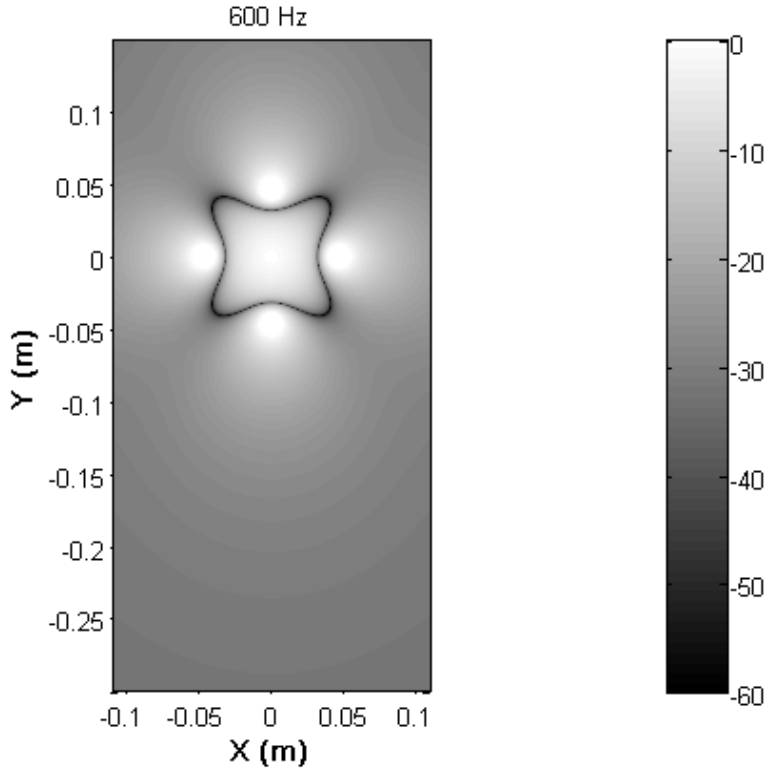

Figure 6. Acoustic pressure field coplanar to the noise and control sources at 600 Hz. The dark line indicates a pressure null demarcating ideal error sensor location.

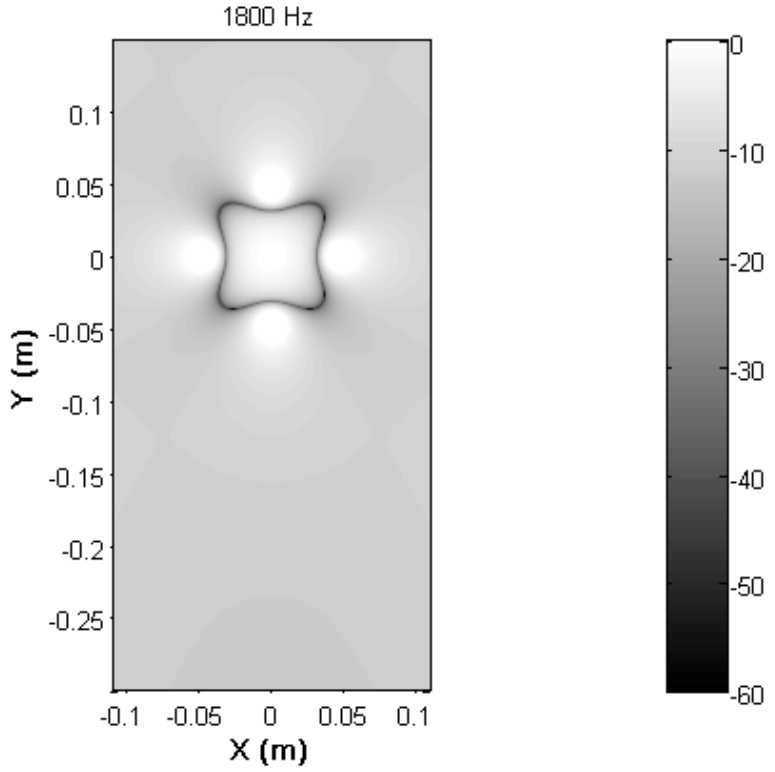

Figure 7. Acoustic pressure field coplanar to the noise and control sources at 1800 Hz.

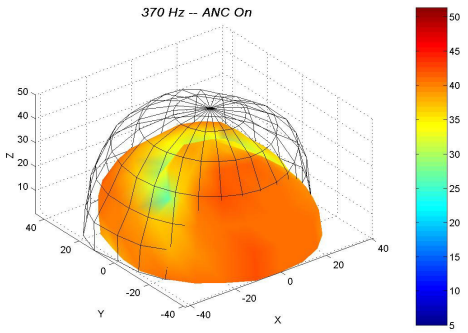

Figure 8.

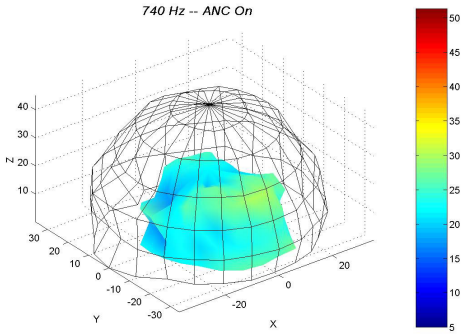

Figure 9.

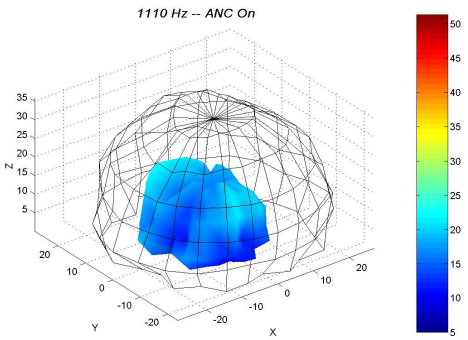

Figure 10.

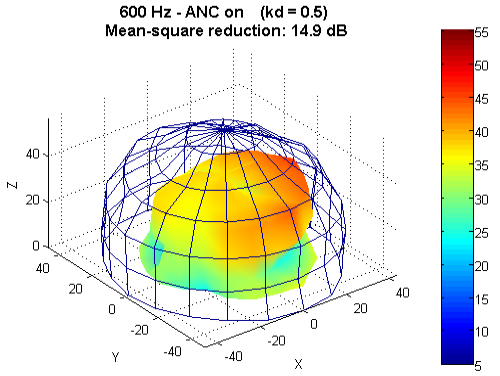

Figure 11.

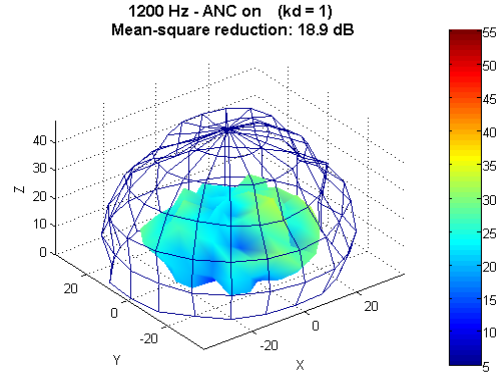

Figure 12.

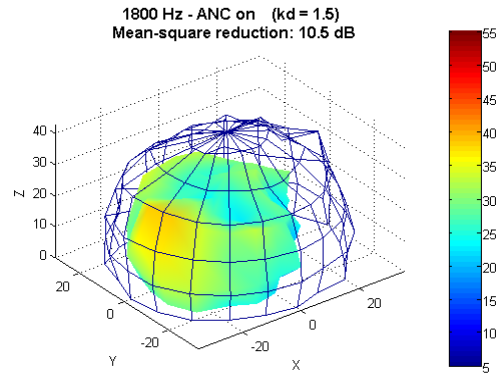

Figure 13.

	80 mm		Ideal		60 mm		Ideal	
	kd	**MPR (dB)**	**kd**	**Predicted**	**kd**	**MPR (dB)**	**kd**	**Predicted**
BPF	0.4	10.1	0.4	~35	0.5	14.9	0.5	~30
2 x BPF	0.8	16.1	0.8	26	1.0	18.9	1.0	22
3 x BPF	1.2	12.8	1.2	18	1.5	10.5	1.5	13.5

Table 1. Overall noise reduction comparison of 80 mm control system, 60 mm control system, and theoretical ideal.